

Immobilization of Proline onto Al-SBA-15 for C–C Bond-Forming Reactions

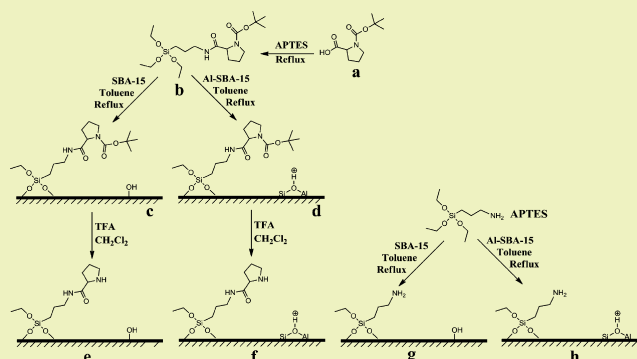
Jingqi Guan,* Bo Liu, Xiaoyuan Yang, Jing Hu, Chunhua Wang, and Qiubin Kan

College of Chemistry, Jilin University, Changchun, 130023, P.R. China

Supporting Information

ABSTRACT: Bifunctionalized materials with different matches of acid and base have been prepared through a post-grafted approach. The synthesized materials were characterized by X-ray diffraction (XRD), nitrogen adsorption–desorption isotherms, XRF analysis, elemental analysis, transmission electron microscopy, IR spectra of pyridine adsorption, thermogravimetry, and CO₂-TPD. The characterization results indicated that the organic amines have been successfully immobilized onto the surface of SBA-15 and Al-SBA-15, and the structure of the supports were kept intact. Moreover, the strength of the acidity for Al-SBA-15 is stronger than that for SBA-15, while the strength of the basicity for tert-butyl 2-(3-(triethoxysilyl)propylcarbamoyl)pyrrolidine-functionalized SBA-15 or Al-SBA-15 is stronger than that for 3-aminopropyltriethoxysilane-functionalized SBA-15 or Al-SBA-15. The synthesized bifunctional acid–base materials were tested in a Knoevenagel reaction, tandem deacetalization–Knoevenagel reaction, one-pot deacetalization–Henry reaction, aldol reaction, and nitroaldol reaction. The catalytic results showed that different acid–base matches favored different reactions.

KEYWORDS: SBA-15, Acid–base, Knoevenagel, Henry, Aldol



INTRODUCTION

Over the past decade, bifunctional materials with acidic and basic properties have received much attention because they can catalyze tandem multistep reactions in one catalytic system or work synergistically to change the characteristics of a single reaction.^{1–11} Direct co-condensation and post-grafting methods have generally been applied for the preparation of these bifunctional materials. Zeidan et al.³ depicted the preparation of acid–base bifunctional SBA-15 with primary amine and different acids (carboxylic, phosphoric, and sulfonic acid) through “one-pot” synthesis and found that higher conversion of the aldol product was achieved when a weaker acid component (carboxylic vs sulfonic) was used. Hicks et al.⁴ put forward a methodology using a protection/deprotection strategy to synthesize base-functionalized SBA-15 with controllable amine spacing and loadings. Our group used two different-sized amino protective groups to prepare two kinds of acid–base bifunctionalized mesoporous SBA-15 materials and found that the steric hindrance of amines with different sizes in the protective groups showed a relationship with the acid–base cooperativity.¹² Zhao et al.¹³ used an acid–base HPA catalyst (C₆H₁₅O₂N₂)₂HPW₁₂O₄₀) for heterogeneous transesterification and esterification reactions. Toyao et al.¹⁴ studied an amino-functionalized metal–organic framework catalyst by using a solvothermal method for a one-pot sequential deacetalization–Knoevenagel condensation reaction. Rostamizadeh et al.¹⁵ investigated the preparation and application of the

magnetic nanocatalyst (α -Fe₂O₃)-MCM-41-L-prolinium nitrate in the production of quinazolin-4(3H)-one derivatives. Hatano et al.¹⁶ have reported that chiral magnesium(II) binaphtholates could be used as cooperative Brønsted/Lewis acid–base catalysts in the highly enantioselective addition of phosphorus nucleophiles to α,β -unsaturated esters and ketones.

Very recently, inorganic acid–base bifunctional materials have been reported and applied in various reactions. For example, Timofeeva et al.¹⁷ synthesized metal phosphate molecular sieves with acid–base properties for the preparation of propylene glycol methyl ether from methanol and propylene oxide. Zhang et al.¹⁸ reported that acid–base bifunctional CaO-ZrO₂ catalysts could be applied in vapor-phase selective dehydration of 1,4-butanediol to 3-buten-1-ol. Sinhamahapatra et al.¹⁹ prepared mesoporous borated zirconia showing high acidity in a Knoevenagel condensation reaction and a Claisen–Schmidt condensation reaction. Li et al.²⁰ produced a core–shell structured MgAl-LDO@Al-MS inorganic nanocomposite with hexagonal Mg–Al mixed oxide nanoplates as the inner core and Al-containing mesoporous silica as the outer shell by a low cost route for one-pot deprotection–Knoevenagel cascade reaction sequences with high activity and selectivity.

Received: December 11, 2013

Revised: January 6, 2014

Published: January 27, 2014

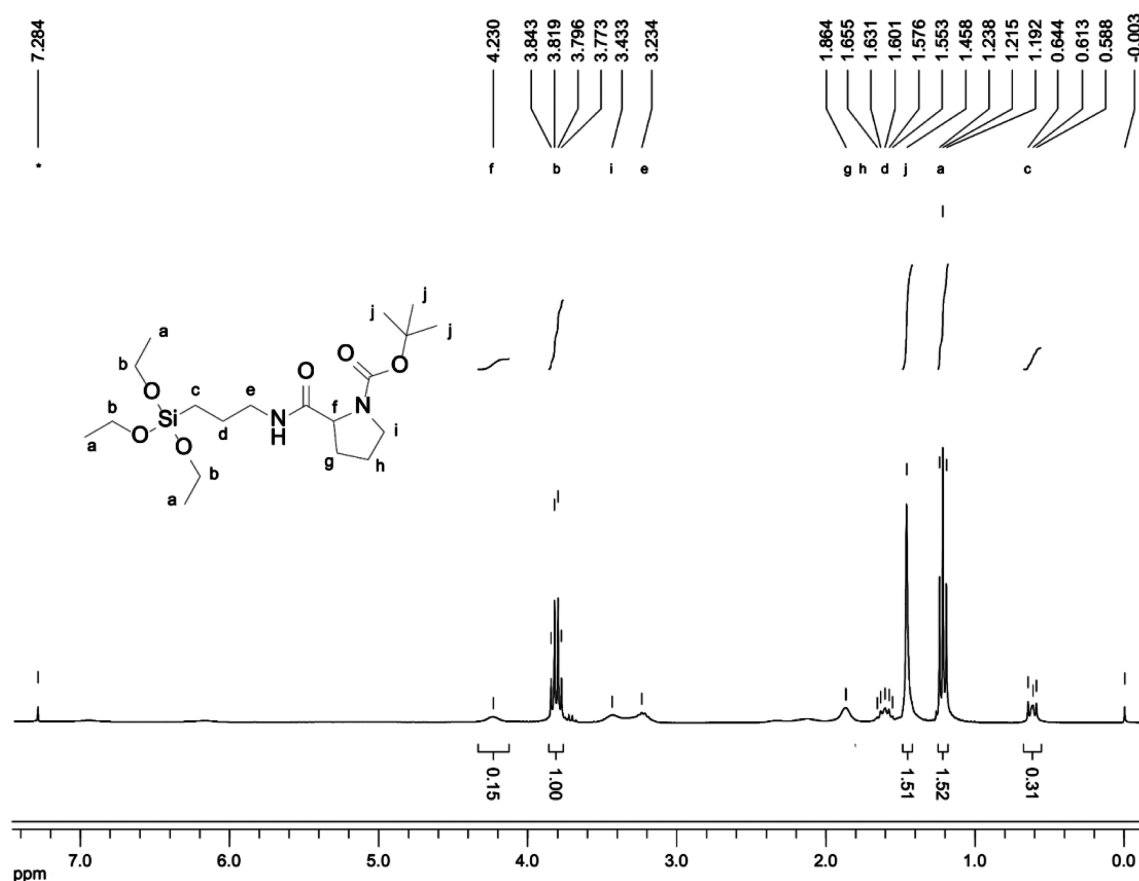


Figure 1. ^1H NMR of tert-butyl 2-(3-(triethoxysilyl)propylcarbamoyl)pyrrolidine-1-carboxylate. * denotes solvent peak.

The past work was mainly concentrated on the adjustment of the acidity of the acid–base bifunctional materials, while the effect of the basicity was seldom investigated. It is well known that the basicity of the materials might have greater influence on some C–C bond-forming reactions than the acidity.^{21,22} The basicity of a primary amino group is usually weaker than that of a secondary amine, and pyrrolidine is usually regarded as a strong base in organic chemistry. Because the proline molecular contains the pyrrolidine group, some researchers used proline and its derivatives as homogeneous catalysts to catalyze diverse reactions or immobilized it onto solid supports to provide base sites.^{2,23–33} For instance, Calderón et al.²³ reported that L-proline heterogenized onto MCM-41 provided stereoselectivities in some cases complementary to the homogeneous catalyst in aldol reactions. Hsiao et al.²⁵ anchored chiral proline derivative on mesoporous SBA-15 materials for asymmetric addition of diethyl zincs to benzaldehydes and found that the catalytic activities may be improved if the catalysts possessed well-distributed and less sterically hindered proline derivatives as well as more hydrophobic surfaces. Khalafi-Nezhad et al.²⁸ supported L-proline on silica to catalyze the one-pot synthesis of spiroindolone derivatives, giving up to 90% yield after reaction for 2 h.

In the current work, bifunctional SBA-15 and Al-SBA-15 catalysts with different acid–base matches were synthesized. The incorporation content of the aluminum and grafted amine amounts are similar for all bifunctionalized materials in order that the catalytic behavior of these materials could be compared to one another.

EXPERIMENTAL SECTION

Catalyst Preparation. SBA-15 silica with a hexagonal p6mm structure was prepared according to the reported procedures^{34,35} using the triblock copolymer Pluronic P123 ($M_{\text{av}} = 5800$, $(\text{EO})_{20}(\text{PO})_{70}(\text{EO})_{20}$, Aldrich) as the structure-directing agent and tetraethyl orthosilicate (TEOS, Aldrich) as the silica source. In a typical synthesis, 2 g of Pluronic P123 copolymer was dissolved in 15 mL of H_2O and 60 mL of 2 M HCl, and then 4.68 mL (0.02 mol) of TEOS was added into the solution under stirring at 313 K. After that, the resultant mixture was stirred at 313 K for 24 h and then aged under static conditions at 373 K for 24 h. Finally, the solid product was recovered by filtration and washed with deionized water. After being air-dried at room temperature overnight, it was calcined at 823 K for 8 h to remove the template. The obtained sample was nominated as SBA-15.

Al-SBA-15 was prepared according to the literatures.^{36,37} In a typical synthesis, 2 g of Pluronic P123 copolymer was dissolved in 75 mL of H_2O , and then 1.92 g $\text{Al}(\text{NO}_3)_3 \cdot 9\text{H}_2\text{O}$ was added and stirred for 0.5 h. Afterward, the mixture was heated to 318 K, and then 4.68 mL (0.02 mol) of TEOS was added. Then, the mixture was stirred at 318 K for 24 h, aged at 373 K for 24 h under static conditions, and then filtered, thoroughly washed, dried, and calcined at 823 K for 8 h to remove the template. The molar composition of the mixture, TEOS/P123/ $\text{Al}(\text{NO}_3)_3/\text{H}_2\text{O}$, was 1/0.017/0.25/192, and the obtained sample was nominated as Al-SBA-15.

Tert-butyl 2-(3-(triethoxysilyl)propylcarbamoyl)pyrrolidine-1-carboxylate was synthesized according to the literature.³⁸ In a typical synthesis, 3.3 mmol of L-proline protected by BOC in the N side and 3.3 mmol of triethylamine were added to 10 mL of dried THF, and then the solution was cooled to 273 K. Afterward, 3.3 mmol of ethyl chloroformate was dropwise added under vigorously stirring. After 30 min, 1 mL of THF containing 4.8 mmol of APTES was introduced into the solution within 15 min. After a further reaction for 1 h, the

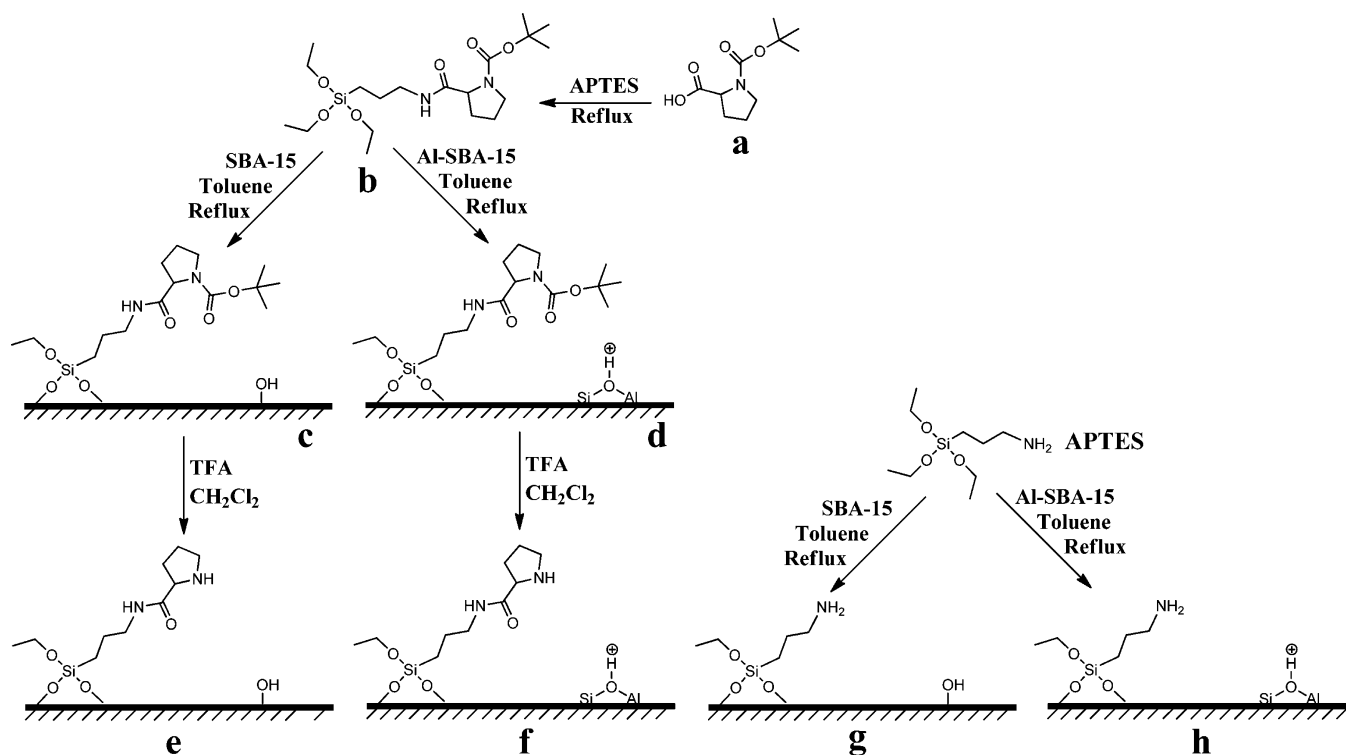


Figure 2. Synthetic route for SBA-15-APTES, Al-SBA-15-APTES, SBA-15-pyrro, and Al-SBA-15-pyrro.

product was successively washed by copious water, saturated NaHCO_3 , and saturated NaCl solution. The organic layer was obtained by a separatory funnel and then dried over MgSO_4 . The resulting solution was concentrated by rotary evaporation under reduced pressure and then filtered through a hexane-packed alumina column. The column was washed with a mixture of hexane/ethyl acetate (7/3). The final product was obtained by evaporating the solvent (^1H NMR in Figure 1 and ^{13}C NMR in Figure S1, Supporting Information).

SBA-15-pyrro-Boc and Al-SBA-15-pyrro-Boc were synthesized as follows (Figure 2).³⁵ A total of 1.0 g of SBA-15 or Al-SBA-15 was refluxed in anhydrous toluene with 0.8 mmol of Tert-butyl 2-(3-(triethoxysilyl)propylcarbamoyl)pyrrolidine-1-carboxylate for 10 h. Then the mixture was filtered and washed abundantly with several solvents with different polarity (hexane, dichloromethane and ethanol) to remove the residual unsupported tert-butyl 2-(3-(triethoxysilyl)propylcarbamoyl)pyrrolidine-1-carboxylate. The obtained solid was dried overnight and nominated as SBA-15-pyrro-Boc and Al-SBA-15-pyrro-Boc.

SBA-15-pyrro and Al-SBA-15-pyrro were synthesized as follows (Figure 2). A total of 1.0 g of SBA-15-pyrro-Boc or Al-SBA-15-pyrro-Boc was first dried under vacuum at 373 K for 5 h and then added into a 50 mL flask containing 10 mL of dried CH_2Cl_2 . After cooling to 273 K, 10 mL of trifluoroacetic acid was dropwise added under N_2 . After that, the mixture was stirred at room temperature for 6 h. Then, the mixture was filtered and washed abundantly with several solvents with different polarity (hexane, dichloromethane, and ethanol) and then washed successively with THF containing 5% triethylamine, copious water, and ethanol until the pH value reached 7. Finally, the solid was obtained by drying at ambient temperature overnight.

SBA-15-APTES and Al-SBA-15-APTES were synthesized by post-synthetic grafting procedures (Figure 2).^{9,35,37} SBA-15 and Al-SBA-15 were first dried under vacuum at 373 K for 5 h. Then 0.5 g of dried SBA-15 or Al-SBA-15 was refluxed in anhydrous toluene with 0.1 mL (0.4 mmol) APTES (3-aminopropyltriethoxysilane) for 10 h. Then, the solid was filtered and washed abundantly with several solvents with different polarity (hexane, dichloromethane, and ethanol) to remove the residual unsupported APTES. The pale solid was dried overnight and nominated as SBA-15-APTES or Al-SBA-15-APTES.

Catalyst Characterization. Powder X-ray diffraction patterns (XRD) were obtained on a Rigaku D/max-2200 ($0.2^\circ/\text{min}$) using Cu K α radiation (40 kV, 40 mA). N_2 adsorption–desorption isotherms were measured with a Micromeritics ASAP 2020 system at liquid N_2 temperature. Before measurements, the sample was outgassed at 403 K for 6 h. The BET surface area was calculated using the Brunauer–Emmett–Teller (BET) method. Transmission electron microscope (TEM) was performed on a Hitachi H-8100 electron microscope operating at 200 kV. Elemental analyses of nitrogen were obtained with a VarioEL CHN elemental analyzer. In situ IR spectra of adsorbed pyridine were recorded on a NICOLET Impact 410 spectrometer. The samples were pressed into self-supporting discs, placed in an IR cell, and treated under vacuum at 473 K for 1 h. Differences in IR spectra were recorded after reaching adsorption/desorption equilibrium of pyridine and evacuating at 373 K for 1 h to remove physically adsorbed pyridine. CO_2 -TPD was measured on a GC-8A, equipped with a thermal conductivity detector. A 100 mg sample was calcined for 1 h at 473 K under a flowing helium gas and then cooled to 323 K to adsorb CO_2 . After, the physically adsorbed CO_2 was purged by a He flow at 323 K, and CO_2 -TPD was performed at the rate of 10 K min^{-1} up to 600 K.

Catalytic Tests. Knoevenagel Reaction. The catalyst (0.05 g), benzene (5 mL), benzaldehyde (1 mmol), and ethyl cyanoacetate (1 mmol) were placed into a reaction vessel.³⁵ The mixture was vigorously stirred at 353 K under nitrogen. After certain times, the catalyst was separated by filtration. The products were analyzed with a BEIFEN-3420A gas chromatograph (GC) equipped with an OV-101 capillary column and FID detector.

One-Pot Deacetalization–Knoevenagel Reaction. Into a reaction vessel were placed the catalyst (0.05 g), benzene (5 mL), benzaldehyde dimethylacetal (1 mmol), and ethyl cyanoacetate (1 mmol).³⁹ The mixture was vigorously stirred at 353 K under nitrogen for 30 min. Then, the catalyst was separated by filtration. The products were analyzed with a BEIFEN-3420A gas chromatograph (GC) equipped with an OV-101 capillary column and FID detector.

One-Pot Deacetalization–Henry Reaction. Into a reaction vessel were placed the catalysts (0.05 g), benzaldehyde dimethylacetal (1.0 mmol), and nitromethane (5 mL).³⁹ The mixture was vigorously stirred at 363 K under nitrogen. The products were analyzed with a

BEIFEN-3420A gas chromatograph (GC) equipped with an OV-101 capillary column and FID detector.

Nitroaldol Reaction. Into a reaction vessel were placed the catalysts (0.05 g), benzaldehyde dimethylacetal (1.0 mmol), and nitromethane (5 mL). The mixture was vigorously stirred at 363 K under nitrogen. The products were analyzed with a BEIFEN-3420A gas chromatograph (GC) equipped with an OV-101 capillary column and FID detector.

Aldol Reaction. Into a reaction vessel were placed the catalysts (0.05 g), 4-nitrobenzaldehyde (1.0 mmol), and acetone (5 mL). The resulting mixture was vigorously stirred at 323 K under nitrogen. The products were analyzed with a BEIFEN-3420A gas chromatograph (GC) equipped with an OV-101 capillary column and FID detector.

RESULTS AND DISCUSSION

The powder XRD patterns of the synthesized SBA-15-APTES, SBA-15-pyrro, Al-SBA-15-APTES, and Al-SBA-15-pyrro are shown in Figure 3. For all of the samples, three well-resolved

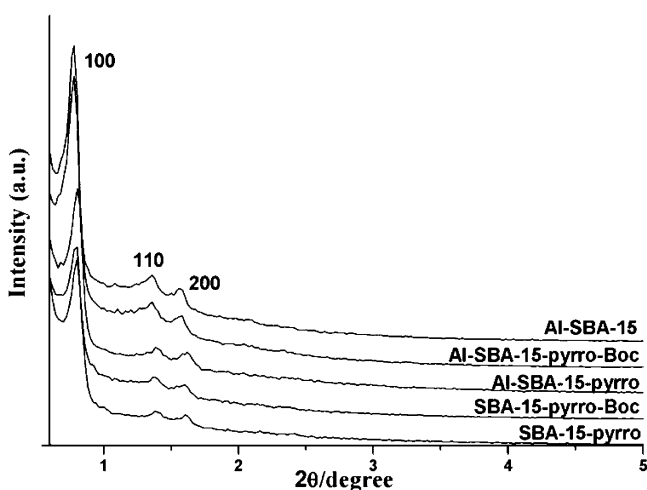


Figure 3. Powder XRD patterns of the synthesized samples.

peaks can be clearly observed, indicating that the prepared bifunctional materials contain well-ordered hexagonal arrays of one-dimensional channel structures.^{12,34}

The TEM images of sample Al-SBA-15-pyrro are presented in Figure 4. Parallel straight pores and hexagonally arrayed pores are clearly observed, which can be ascribed to the (110) and (100) directions of the $p6mm$ phase, respectively.^{12,34} TEM images indicate that the structural ordering of Al-SBA-15-pyrro remains intact after the organic modifications. This result,

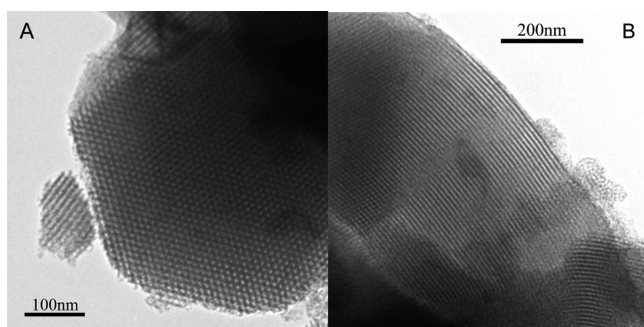


Figure 4. TEM images of Al-SBA-15-pyrro in the direction of the pore axis (A) and in the direction perpendicular to the pore axis (B).

together with the XRD patterns, confirms the formation of the highly ordered mesostructure.

The N_2 adsorption–desorption isotherms of Al-SBA-15-pyrro, SBA-15-APTES, Al-SBA-15, and SBA-15 are shown in Figure 5, and BJH pore size distributions of Al-SBA-15-pyrro

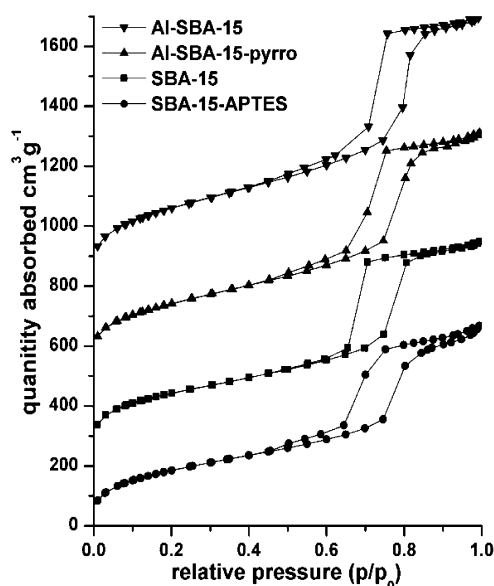


Figure 5. N_2 adsorption–desorption isotherms of Al-SBA-15-pyrro, SBA-15-APTES, Al-SBA-15, and SBA-15.

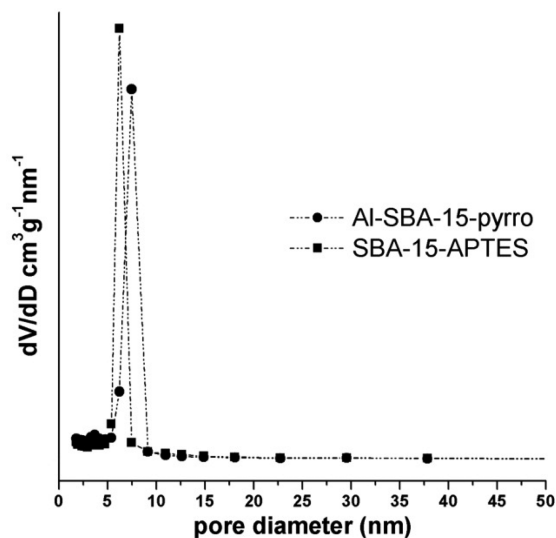


Figure 6. BJH pore size distributions of Al-SBA-15-pyrro and SBA-15-APTES.

and SBA-15-APTES are represented in Figure 6. It is shown that the four samples display a type IV isotherm with H1 hysteresis and a sharp increase in volume adsorbed in the P/P_0 range from 0.6 to 0.8, indicating that the ordered mesoporous structure of SBA-15 is well remained.¹² From Table 1, it is observed that after the introduction of organic functional groups, the BET specific surface area gradually decreases from 831 m^2/g for SBA-15 to 648 m^2/g for SBA-15-APTES and from 904 m^2/g for Al-SBA-15 to 746 m^2/g for Al-SBA-15-

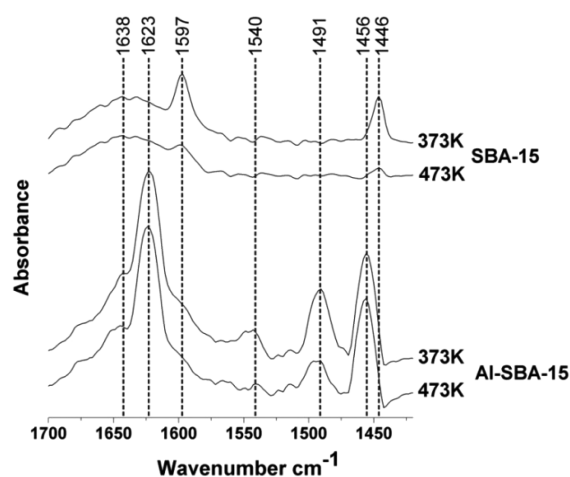
Table 1. Structural and Textural Parameters of the Synthesized Materials

sample	S_{BET}^a ($\text{m}^2 \text{g}^{-1}$)	D_p^b (nm)	V_p^c ($\text{cm}^3 \text{g}^{-1}$)
SBA-15	831	5.8	1.18
SBA-15-APTES	648	5.7	1.05
Al-SBA-15	904	6.3	1.36
Al-SBA-15-pyrro	746	6.1	1.19

$^a S_{\text{BET}}$ = surface area. $^b D_p$ = average pore width. $^c V_p$ = total pore volume.

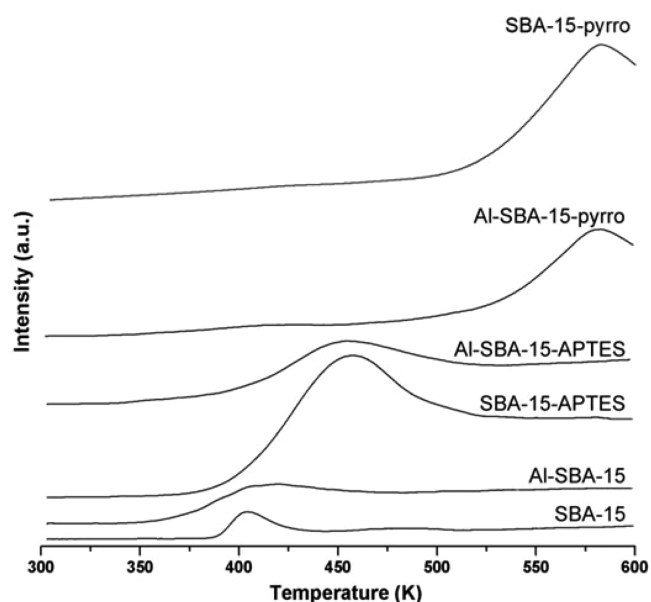
pyrro. In addition, the pore diameter and total pore volume decrease slightly after the functionalization of SBA-15 or Al-SBA-15.

The surface acidity of SBA-15 and Al-SBA-15 was examined through pyridine adsorption and subsequent IR spectroscopy (Figure 7). Al-SBA-15 gives two IR bands at 1456 and 1623

**Figure 7.** IR spectra of pyridine adsorption on SBA-15 and Al-SBA-15 at 373 K and 473 K.

cm^{-1} due to pyridine adsorbed on Lewis acid sites, two IR bands at 1540 and 1638 cm^{-1} due to pyridine adsorbed on Brønsted acid sites, and one band at 1491 cm^{-1} attributed to pyridine associated with both Lewis and Brønsted acid sites. However, these peaks are very weak for pure silica SBA-15, indicating that its acidity is far weaker than Al-SBA-15.

The surface basicity of Al-SBA-15-pyrro, Al-SBA-15-APTES, SBA-15-APTES, Al-SBA-15, and SBA-15 was examined through CO_2 -TPD spectra (Figure 8). Because the pyrrolidine and APTES grafted onto SBA-15 are more stable than the corresponding pure organic compounds,⁴⁰ which could bear up to about 600 K and do not decompose (Figure S2, Supporting Information), the TPD experiment was carried out from room temperature to 600 K.⁴¹ It is shown that the absorption peaks for Al-SBA-15 and SBA-15 are centered at about 405 K indicating the existence of weak basic sites in the two materials. Moreover, there is an absorption peak centered at about 460 and 580 K for Al-SBA-15-APTES and Al-SBA-15-pyrro, respectively, indicating that the organic amine has been successfully grafted onto Al-SBA-15, and the basicity of Al-SBA-15-pyrro is stronger than that of Al-SBA-15-APTES. In addition, the absorption peak position of SBA-15-APTES (or SBA-15-pyrro) is the same as that of Al-SBA-15-APTES (or Al-SBA-15-pyrro), while the peak area of the former is larger than the latter, indicating that there is the same basicity in the two

**Figure 8.** CO_2 -TPD spectra of SBA-15-pyrro, Al-SBA-15-pyrro, Al-SBA-15-APTES, SBA-15-APTES, Al-SBA-15, and SBA-15.

couple materials, while the different acidity of the supports might have influence on the CO_2 adsorbing capacity. In addition, there is no absorption peak for SBA-15-pyrro and Al-SBA-15-pyrro under 500 K, suggesting no weak base sites in the bifunctional materials.

Quantification of the functional group loaded in SBA-15 and Al-SBA-15 was performed for the bifunctional materials using elemental analysis (CHN) (Table 2). The results of CHN elemental analysis indicate that there is very little difference in the amount of basic groups grafted onto the surface of SBA-15 and Al-SBA-15.

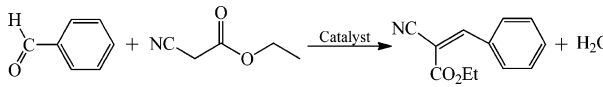
Table 2. Analytical Data for Prepared Materials

sample	amount of base groups ^a (mmol g^{-1})	Al ^b (%)	Si/Al ^b
SBA-15-pyrro	0.31	—	—
Al-SBA-15-pyrro	0.29	1.532	25
SBA-15-APTES	0.27	—	—
Al-SBA-15-APTES	0.28	1.567	25

^aAmount of base groups grafted onto the surface was calculated from elemental analysis. ^bAmount of aluminum species and Si/Al ratio were calculated from XRF analysis.

The catalytic properties of the bifunctionalized materials in the Knoevenagel reaction are shown in Table 3. It is shown that the catalytic activity over weak base catalysts (SBA-15-APTES and Al-SBA-15-APTES) is much better than that over strong base catalysts (SBA-15-pyrro and Al-SBA-15-pyrro). In addition, the catalytic performance of catalysts with weak acid (SBA-15-APTES and SBA-15-pyrro) is also better than the catalytic performance of catalysts with moderately strong acid and the same base (Al-SBA-15-APTES and Al-SBA-15-pyrro). In general, weak acid matching weak base favors the Knoevenagel reaction. Moreover, the catalyst SBA-15-APTES can be reused three times without significant loss of the activity.

Parvin et al.⁴² reported imidazolium chloride-immobilized SBA-15 for solvent-free Knoevenagel condensation using a microwave and found that the acid–base-bifunctionalized SBA-

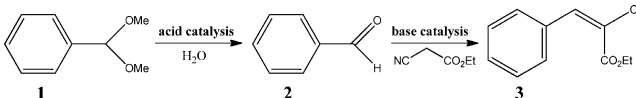
Table 3. Reaction Data for Knoevenagel Reaction over Different Catalysts^a


catalyst	conversion (%)	selectivity (%)
SBA-15	<1	–
Al-SBA-15	<1	–
SBA-15-APTES (first)	94.7	~100
SBA-15-APTES (second)	94.5	~100
SBA-15-APTES (third)	94.6	~100
Al-SBA-15-APTES	76.7	~100
SBA-15-pyrro	44.0	~100
Al-SBA-15-pyrro	35.4	~100

^aReaction conditions: benzaldehyde (1 mmol), ethyl cyanoacetate (1 mmol), catalyst (0.05 g). Reaction time: 30 min. Reaction temperature: 353 K.

15 with a 7.5% base group performed very well. Motokura et al.⁴³ also reported that an acid–base bifunctional catalyst SA-supported 3-(diethylamino)propyl functional group (SANET₂) possessed high catalytic performance in the addition reaction of ethyl cyanoacetate to methyl vinyl ketone, affording up to 90% yield of 2-cyano-5-oxo-2-(3-oxobutyl)hexanoic acid ethyl ester, while both triethylamine and amorphous silica–alumina (SA) showed no catalytic activity. In addition, Almeida and Cardoso⁴⁴ found that the catalytic activity of (CH₃)₃NH⁺ and (CH₃)₄N⁺ ions-exchanged Y zeolites (Me₃Y and Me₄Y) was obviously lower than that of CH₃CH₂CH₂NH₃⁺ and CH₃CH₂CH₂CH₂NH₃⁺ ions-exchanged Y zeolites (Pr₁Y and Bu₁Y) in the Knoevenagel condensation of n-butyraldehyde with ethyl cyanoacetate, although the Me₃⁺ and Me₄⁺ cations provided higher basicity.

The catalytic properties of the bifunctionalized materials in the one-pot deacetalization–Knoevenagel reaction are listed in Table 4. The first reaction step is the acid-catalyzed deacetalization of dimethoxymethylbenzene to give benzaldehyde, while the second reaction step is the base-catalyzed Knoevenagel reaction to give the final product benzylidene ethyl cyanoacetate. It can be inferred that catalysts with weak acid and weak base (e.g., SBA-15-APTES) cannot efficiently catalyze this reaction. Moreover, catalysts only with moderately

Table 4. Reaction Data for One-Pot Deacetalization–Knoevenagel Reaction over Different Catalysts^a


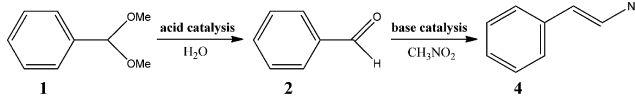
catalyst	conversion of 1 (%)	yield of 2 (%)	yield of 3 (%)
SBA-15-APTES	trace	–	–
Al-SBA-15-APTES (first)	75.2	2.5	72.7
Al-SBA-15-APTES (second)	74.9	2.3	72.6
Al-SBA-15-APTES (third)	74.6	2.3	72.7
SBA-15	trace	trace	–
Al-SBA-15	11.4	11.4	–
Al-SBA-15-pyrro	14.2	7.3	6.9

^aReaction conditions: **1** (1 mmol), ethyl cyanoacetate (1 mmol), catalyst (0.05 g). Reaction time: 30 min. Reaction temperature: 353 K.

strong acid (e.g., Al-SBA-15) cannot catalyze the second reaction needing base catalysis. Additionally, catalysts with moderately strong acid and strong base (i.e., Al-SBA-15-pyrro) cannot also effectively catalyze the one-pot tandem deacetalization–Knoevenagel reaction. Indeed, relatively high catalytic activity can be observed over Al-SBA-15-APTES with moderately strong acid and weak base with 75.2% conversion of **1** and 72.7% yield of **3**. Furthermore, only a negligible deactivation occurs for the catalyst Al-SBA-15-APTES after being used three times. The slight decrease in conversion is probably due to the incomplete removal of absorbed species from the active sites.

Motokura et al.⁴⁵ described an interesting phenomenon in the tandem deacetalization–Knoevenagel condensation over organic primary amines immobilized onto acidic montmorillonite interlayers (H-mont-NH₂). They found that the preparation solvents have a great influence on the catalytic activities. For example, the catalyst prepared in heptane (H-mont-NH₂ [heptane]) gave >99% conversion of dimethoxymethylbenzene and >95% yield of the final product **3**, while the catalytic behavior over the catalysts synthesized in THF, toluene, DMSO, acetonitrile, and water was much worse than that of H-mont-NH₂ [heptane]. In addition, they also found that the catalytic performance over acidic montmorillonite interlayers (H-mont) was worse than that of H-mont-NH₂ [heptane]. The former only afforded 26% conversion of dimethoxymethylbenzene and trace yield of the final product **3** after reaction for 1 h. It is similar with our experimental results. As mentioned above, the catalytic behavior of the acidic catalyst Al-SBA-15 is worse than the acid–base bifunctional catalysts Al-SBA-15-pyrro and Al-SBA-15-APTES. A reasonable explanation for the phenomenon might be that the existence of base in the catalysts favors the transformation of the intermediate product **2** and thus accelerates the reaction. As for the catalytic behavior of Al-SBA-15-pyrro, it is far worse than that of Al-SBA-15-APTES; weak bases might better catalyze the second base-catalyzed Knoevenagel reaction than strong bases.

The catalytic properties of the bifunctionalized materials in the one-pot deacetalization–Henry reaction are presented in Table 5. The weak acid catalyst SBA-15 shows no catalytic activity, while the catalyst with weak acid and weak base also cannot catalyze this reaction. Moreover, the catalyst with moderately strong acid (Al-SBA-15) affords very low conversion of **1** and no final product due to the lack of base sites, while the catalyst with moderately strong acid and strong

Table 5. Reaction Data for One-Pot Deacetalization–Henry Reaction over Different Catalysts^a


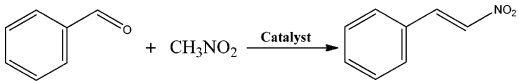
catalyst	conversion of 1 (%)	yield of 2 (%)	yield of 4 (%)
SBA-15	trace	–	–
Al-SBA-15	2.1	2.1	–
SBA-15-APTES	trace	–	–
Al-SBA-15-APTES	38.4	4.4	34
SBA-15-pyrro	trace	–	–
Al-SBA-15-pyrro	4.7	0.8	3.9

^aReaction conditions: **1** (1 mmol), nitromethane (5 mL), catalyst (0.05 g). Reaction time: 30 min. Reaction temperature: 363 K.

base can give 3.9% yield of the final product **4**. Although the acidity of Al-SBA-15 might be stronger than that of Al-SBA-15-pyrro, the existence of base in Al-SBA-15-pyrro could favor the transformation of the intermediate product **2** and thus properly accelerate the cascade reaction. In addition, the catalyst with moderately strong acid and weak base favors the tandem reaction. In the case of the Henry reaction, it is difficult to achieve high selectivity of the nitroalkene using strong bases because the conjugate addition of the nitroalkane to form bis-nitro compounds in a side reaction. Thereby, the synthesis of nitroalkene over strong base catalysts often proceeds in poor yield due to the dimerization or polymerization.^{11,46,47}

The catalytic properties of the bifunctionalized materials in the nitroaldol reaction are described in Table 6. Base-free

Table 6. Reaction Data for Nitroaldol Reaction over Different Catalysts^a



catalyst	conversion (%)	selectivity (%)
SBA-15	trace	–
Al-SBA-15	trace	–
SBA-15-APTES	~100	~100
Al-SBA-15-APTES	65.5	~100
SBA-15-pyrro	15.8	~100
Al-SBA-15-pyrro	8.9	~100

^aReaction conditions: benzaldehyde (1 mmol), nitromethane (5 mL), catalyst (0.05 g). Reaction time: 30 min. Reaction temperature: 363 K.

catalysts SBA-15 and Al-SBA-15 cannot catalyze this nitroaldol reaction of benzaldehyde and nitromethane at all, while acid–base bifunctional catalysts can catalyze this reaction. Furthermore, the catalytic activity over the four bifunctionalized catalysts is as follows: SBA-15-APTES > Al-SBA-15-APTES > SBA-15-pyrro > Al-SBA-15-pyrro. Therefore, it is supposed that strong base is not very suitable for the nitroaldol reaction. Catalysts with weak acid and weak base (e.g., SBA-15-APTES) can catalyze this reaction with nearly 100% yield.

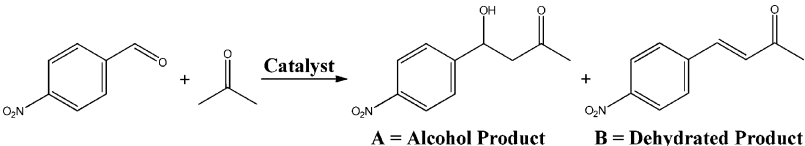
Shylesh et al.⁴⁸ reported an acid–base bifunctional catalyst MSN–NNH₂–SO₃H with strong acid and weak base for the nitroaldol reaction and found that 89% yield of the nitroalkene

product can be achieved after reaction for 6 h. However, our prepared SBA-15-APTES only needs 30 min to complete this reaction. They also found that catalysts without base sites (e.g., MSN and MSN–SO₃H) displayed no catalytic activity at all.

The catalytic properties of the bifunctionalized materials in the aldol reaction of acetone with 4-nitrobenzaldehyde are summarized in Table 7. It is clear that catalysts without base sites (SBA-15 and Al-SBA-15) or catalysts with protected base sites (e.g., SBA-15-pyrro-Boc and Al-SBA-15-pyrro-Boc) cannot catalyze the aldol reaction. The catalytic activity over the four bifunctionalized catalysts is as follows: Al-SBA-15-APTES (moderately strong acid and weak base) > SBA-15-pyrro (weak acid and strong base) > Al-SBA-15-pyrro (moderately strong acid and strong base) > SBA-15-APTES (weak acid and weak base). In addition, the product distribution is also affected by the acidity and basicity of the catalysts. Basically, the ratio of alcohol product to dehydrated product is higher over catalysts with stronger acidity.

Davis and co-workers^{3,49} synthesized acid–base bifunctional SBA-15 incorporated with primary amine and different acids (sulfonic acid, phosphoric acid, and carboxylic acid) for an aldol reaction of acetone with 4-nitrobenzaldehyde. They found the carboxylic acid/amine material showed highest catalytic activity, followed by the phosphoric acid/amine catalyst, while the combination of sulfonic acid with amines was the worst. In addition, the same authors also found that the product A/B molar ratio was the highest over the phosphoric acid/amine catalyst with moderately strong acid and weak base, followed by the carboxylic acid/amine catalyst. Brunelli et al.⁵⁰ prepared a series of aminosilanes grafted onto mesoporous SBA-15 silica with controlled linker lengths including C1 (methyl), C2 (ethyl), C3 (propyl), C4 (butyl), and C5 (pentyl). In the aldol condensation of 4-nitrobenzaldehyde and acetone, the reaction rate increased with the number of carbons in the carbon chain up to the propyl chain. They also suggested that the interaction between amines and silanols should be weaker than that between amines and carboxylic acids, especially between proline and carboxylic acids.⁵¹ Our group optimized the synergetic effect between the acidic and basic groups by finely tuning the distance between the two kinds of groups and found that it was an important factor influencing the catalytic behavior.³⁷

Table 7. Reaction Data for Aldol Reaction over Different Catalysts^a



catalyst	conversion (%)	A ^b (%)	B ^b (%)	A/B	TOF (mol/site/h)
SBA-15-APTES	21.1	86.8	13.2	6.6	0.84
Al-SBA-15-APTES	54.7	91.6	8.4	10.9	2.18
SBA-15-pyrro	47.5	84.1	15.9	5.3	1.89
Al-SBA-15-pyrro	26.0	94.5	5.5	17.1	1.04
SBA-15	trace	–	–	–	–
Al-SBA-15	trace	–	–	–	–
SBA-15-pyrro-Boc	trace	–	–	–	–
Al-SBA-15-pyrro-Boc	trace	–	–	–	–

^aReaction conditions: 4-nitrobenzaldehyde (1 mmol), acetone (5 mL), catalyst (0.05 g). Reaction time: 30 min. Reaction temperature: 323 K.

^bSelectivity calculated through ¹H NMR spectroscopic analysis.

CONCLUSIONS

In this study, a series of acid–base bifunctional catalysts with different matches of acidity and basicity were prepared. XRD data provide evidence that the functionalized materials keep a 2D-hexagonal mesoporous framework. TEM profiles show the formation of the highly ordered mesostructure. Elemental analysis and IR spectra of pyridine adsorption confirm that the aluminum species and the base groups are successfully incorporated onto the mesoporous SBA-15. The synergic effect between the acid and base in the bifunctional materials is observed. In our tested conditions, weak acid matching weak base is beneficial to the Knoevenagel reaction and nitroaldol reaction, while moderately strong acid matching weak base is advantageous to the one-pot deacetalization–Knoevenagel reaction, one-pot deacetalization–Henry reaction, and aldol reaction.

ASSOCIATED CONTENT

Supporting Information

¹³C NMR of tert-butyl 2-(3-(triethoxysilyl)propylcarbamoyl)-pyrrolidine-1-carboxylate and TG profiles of SBA-15, SBA-15-APTES, and SBA-15-pyrro. This material is available free of charge via the Internet at <http://pubs.acs.org>.

AUTHOR INFORMATION

Corresponding Author

*E-mail: guanjq@jlu.edu.cn (J.G.).

Notes

The authors declare no competing financial interest.

ACKNOWLEDGMENTS

This work was supported by the National Natural Science Foundation of China (21303069) and Jilin province (201105006).

REFERENCES

- (1) Saito, S.; Yamamoto, H. Design of acid–base catalysis for the asymmetric direct aldol reaction. *Acc. Chem. Res.* **2004**, *37*, 570–579.
- (2) Hoang, L.; Bahmanyar, S.; Houk, K.; List, B. Kinetic and stereochemical evidence for the involvement of only one proline molecule in the transition states of proline-catalyzed intra- and intermolecular aldol reactions. *J. Am. Chem. Soc.* **2003**, *125*, 16–17.
- (3) Zeidan, R. K.; Davis, M. E. The effect of acid–base pairing on catalysis: An efficient acid–base functionalized catalyst for aldol condensation. *J. Catal.* **2007**, *247*, 379–382.
- (4) Hicks, J. C.; Dabestani, R.; Buchanan, A.; Jones, C. W. Spacing and site isolation of amine groups in 3-aminopropyl-grafted silica materials: The role of protecting groups. *Chem. Mater.* **2006**, *18*, 5022–5032.
- (5) Margelefsky, E. L.; Zeidan, R. K.; Davis, M. E. Cooperative catalysis by silica-supported organic functional groups. *Chem. Soc. Rev.* **2008**, *37*, 1118–1126.
- (6) Hruby, S. L.; Shanks, B. H. Acid–base cooperativity in condensation reactions with functionalized mesoporous silica catalysts. *J. Catal.* **2009**, *263*, 181–188.
- (7) Shylesh, S.; Thiel, W. R. Bifunctional acid–base cooperativity in heterogeneous catalytic reactions: Advances in silica supported organic functional groups. *ChemCatChem* **2011**, *3*, 278–287.
- (8) Paull, D. H.; Abraham, C. J.; Scerba, M. T.; Alden-Danforth, E.; Lectka, T. Bifunctional asymmetric catalysis: Cooperative Lewis acid/base systems. *Acc. Chem. Res.* **2008**, *41*, 655–663.
- (9) Margelefsky, E. L.; Bendjérou, A.; Zeidan, R. K.; Dufaud, V.; Davis, M. E. Nanoscale organization of thiol and arylsulfonic acid on

silica leads to a highly active and selective bifunctional, heterogeneous catalyst. *J. Am. Chem. Soc.* **2008**, *130*, 13442–13449.

- (10) Jun, S. W.; Shokouhimehr, M.; Lee, D. J.; Jang, Y.; Park, J.; Hyeon, T. One-pot synthesis of magnetically recyclable mesoporous silica supported acid–base catalysts for tandem reactions. *Chem. Commun.* **2013**, *49*, 7821–7823.

- (11) Gianotti, E.; Diaz, U.; Velty, A.; Corma, A. Designing bifunctional acid-base mesoporous hybrid catalysts for cascade reactions. *Catal. Sci. Technol.* **2013**, *3*, 2677–2688.

- (12) Shao, Y.; Guan, J.; Wu, S.; Liu, H.; Liu, B.; Kan, Q. Synthesis, characterization and catalytic activity of acid-base bifunctional materials by controlling steric hindrance. *Microporous Mesoporous Mater.* **2010**, *128*, 120–125.

- (13) Zhao, Q.; Wang, H.; Zheng, H.; Sun, Z.; Shi, W.; Wang, S.; Wang, X.; Jiang, Z. Acid-base bifunctional HPA nanocatalysts promoting heterogeneous transesterification and esterification reactions. *Catal. Sci. Technol.* **2013**, *3*, 2204–2209.

- (14) Toyao, T.; Fujiwaki, M.; Horiuchi, Y.; Matsuoka, M. Application of an amino-functionalised metal-organic framework: an approach to a one-pot acid–base reaction. *RSC Adv.* **2013**, *3*, 21582–21587.

- (15) Rostamizadeh, S.; Nojavan, M.; Aryan, R.; Isapoor, E.; Azad, M. Amino acid-based ionic liquid immobilized on alpha-Fe₂O₃-MCM-41: An efficient magnetic nanocatalyst and recyclable reaction media for the synthesis of quinazolin-4(3H)-one derivatives. *J. Mol. Catal. A: Chem.* **2013**, *374*, 102–110.

- (16) Hatano, M.; Horibe, T.; Ishihara, K. Chiral magnesium(II) binaphtholates as cooperative Bronsted/Lewis acid–base catalysts for the highly enantioselective addition of phosphorus nucleophiles to alpha,beta-unsaturated esters and ketones. *Angew. Chem., Int. Ed.* **2013**, *52*, 4549–4553.

- (17) Timofeeva, M. N.; Panchenko, V. N.; Jun, J. W.; Hasan, Z.; Kikhtyanin, O. V.; Prosvirin, I. P.; Jung, S. H. Effect of the acid-base properties of metal phosphate molecular sieves on the catalytic performances in synthesis of propylene glycol methyl ether from methanol and propylene oxide. *Microporous Mesoporous Mater.* **2013**, *165*, 84–91.

- (18) Zhang, Q.; Zhang, Y.; Li, H.; Gao, C.; Zhao, Y. Heterogeneous CaO-ZrO₂ acid–base bifunctional catalysts for vapor-phase selective dehydration of 1,4-butanediol to 3-buten-1-ol. *Appl. Catal., A* **2013**, *466*, 233–239.

- (19) Sinhamahapatra, A.; Pal, P.; Tarafdar, A.; Bajaj, H. C.; Panda, A. B. Mesoporous borated zirconia: A solid acid-base bifunctional catalyst. *ChemCatChem* **2013**, *5*, 331–338.

- (20) Li, P.; Yu, Y.; Huang, P.-P.; Liu, H.; Cao, C.-Y.; Song, W.-G. Core-shell structured MgAl-LDO@Al-MS hexagonal nanocomposite: an all inorganic acid-base bifunctional nanoreactor for one-pot cascade reactions. *J. Mater. Chem. A* **2014**, *2*, 339–344.

- (21) Mukherjee, S.; Yang, J. W.; Hoffmann, S.; List, B. Asymmetric enamine catalysis. *Chem. Rev.* **2007**, *107*, 5471–5569.

- (22) Notz, W.; Tanaka, F.; Barbas, C. F. Enamine-based organo-catalysis with proline and diamines: the development of direct catalytic asymmetric Aldol, Mannich, Michael, and Diels-Alder reactions. *Acc. Chem. Res.* **2004**, *37*, 580–591.

- (23) Calderón, F.; Fernández, R.; Sánchez, F. Fernández-Mayoralas, A. Asymmetric aldol reaction using immobilized proline on mesoporous support. *Adv. Synth. Catal.* **2005**, *347*, 1395–1403.

- (24) Goren, K.; Kehat, T.; Portnoy, M. Elucidation of Architectural Requirements from a Spacer in Supported Proline-Based Catalysts of Enantioselective Aldol Reaction. *Adv. Synth. Catal.* **2009**, *351*, 59–65.

- (25) Hsiao, L.-H.; Chen, S.-Y.; Huang, S.-J.; Liu, S.-B.; Chen, P.-H.; Chan, J. C.-C.; Cheng, S. Enantioselective addition of diethylzinc to benzaldehyde over mesoporous SBA-15 functionalized with chiral proline derivatives. *Appl. Catal., A* **2009**, *359*, 96–107.

- (26) Indumathi, S.; Menendez, J. C.; Perumal, S. L-Proline catalyzed domino reactions for the synthesis of heterocycles. *Curr. Org. Chem.* **2013**, *17*, 2038–2064.

- (27) Thingom, B.; Moirangthem, S. D.; Laitonjam, W. S. Cadmium–proline catalyzed direct asymmetric Michael and aldol reactions in water. *Indian J. Chem. B* **2013**, *52*, 929–936.

- (28) Khalafi-Nezhad, A.; Shahidzadeh, E. S.; Sarikhani, S.; Panahi, F. A new silica-supported organocatalyst based on L-proline: An efficient heterogeneous catalyst for one-pot synthesis of spiroindolones in water. *J. Mol. Catal. A: Chem.* **2013**, *379*, 1–8.
- (29) Nagata, K.; Kuga, Y.; Higashi, A.; Kinoshita, A.; Kanemitsu, T.; Miyazaki, M.; Itoh, T. Asymmetric synthesis and catalytic activity of 3-methyl-beta-proline in enantioselective anti-Mannich-type reactions. *J. Org. Chem.* **2013**, *78*, 7131–7136.
- (30) Biswas, S.; Jaiswal, P. K.; Singh, S.; Mobin, S. M.; Samanta, S. L-Proline catalyzed stereoselective synthesis of (E)-methyl-alpha-indol-2-yl-beta-aryl/alkyl acrylates: Easy access to substituted carbazoles, gamma-carbolines and prenostodione. *Org. Biomol. Chem.* **2013**, *11*, 7084–7087.
- (31) Liu, B.; Li, X.; Zhang, J.; Chmielewski, P. J. L-Proline catalyzed reaction of N-confused porphyrin and active methylene compounds. *Org. Biomol. Chem.* **2013**, *11*, 4831–4839.
- (32) He, T.; Li, K.; Wu, M.-Y.; Wu, M.-B.; Wang, N.; Pu, L.; Yu, X.-Q. Water promoted enantioselective aldol reaction by proline-cholesterol and -diosgenin based amphiphilic organocatalysts. *Tetrahedron* **2013**, *69*, 5136–5143.
- (33) Dandia, A.; Jain, A. K.; Laxkar, A. K.; Bhati, D. S. A highly efficient protocol for the regio- and stereo-selective synthesis of spiro pyrrolidine and pyrrolizidine derivatives by multicomponent reaction. *Tetrahedron Lett.* **2013**, *54*, 3180–3184.
- (34) Zhao, D.; Huo, Q.; Feng, J.; Chmelka, B. F.; Stucky, G. D. Nonionic triblock and star diblock copolymer and oligomeric surfactant syntheses of highly ordered, hydrothermally stable, mesoporous silica structures. *J. Am. Chem. Soc.* **1998**, *120*, 6024–6036.
- (35) Wang, C.; Shang, F.; Yu, X.; Guan, J.; Kan, Q. Synthesis of bifunctional catalysts Al-SBA-15-NH₂ with high aluminum content and the catalytic application for different one-pot reactions. *Appl. Surf. Sci.* **2012**, *258*, 6846–6852.
- (36) Wu, Z. Y.; Wang, H. J.; Zhuang, T. T.; Sun, L. B.; Wang, Y. M.; Zhu, J. H. Multiple functionalization of mesoporous silica in one-pot: Direct synthesis of aluminum-containing plugged SBA-15 from aqueous nitrate solutions. *Adv. Funct. Mater.* **2008**, *18*, 82–94.
- (37) Liu, B.; Liu, H.; Wang, C.; Liu, L.; Wu, S.; Guan, J.; Kan, Q. Exploration of acid-base geometric influence on cooperative activation for aldol reaction. *Appl. Catal. A-Gen.* **2012**, *443*, 1–7.
- (38) Corma, A.; Iglesias, M.; Mohino, F.; Sánchez, F. Heterogenized catalysts on zeolites. Synthesis of new chiral Rh(I) complexes with (2S,4R)-trans-4-RCOO-2-(t-butylaminocarbonyl) pyrrolidines and (2S,4S)-cis-4-RCONH-2-(t-butylaminocarbonyl) pyrrolidines. Heterogenisation on silica and a USY-zeolite and study of the role of support on their catalytic profile in hydrogenation of olefins. *J. Organomet. Chem.* **1997**, *544*, 147–156.
- (39) Shang, F.; Sun, J.; Wu, S.; Yang, Y.; Kan, Q.; Guan, J. Direct synthesis of acid-base bifunctional mesoporous MCM-41 silica and its catalytic reactivity in deacetalization–Knoevenagel reactions. *Microporous Mesoporous Mater.* **2010**, *134*, 44–50.
- (40) Goel, N.; Singh, U. P. Syntheses, structural, computational, and thermal analysis of acid–base complexes of picric acid with N-heterocyclic bases. *J. Phys. Chem. A* **2013**, *117*, 10428–10437.
- (41) Shang, F.; Sun, J.; Wu, S.; Liu, H.; Guan, J.; Kan, Q. Direct synthesis of acid–base bifunctionalized hexagonal mesoporous silica and its catalytic activity in cascade reactions. *J. Colloid Interface Sci.* **2011**, *355*, 190–197.
- (42) Parvin, M. N.; Jin, H.; Ansari, M. B.; Oh, S.-M.; Park, S.-E. Imidazolium chloride immobilized SBA-15 as a heterogenized organocatalyst for solvent free Knoevenagel condensation using microwave. *Appl. Catal. A-Gen.* **2012**, *413*, 205–212.
- (43) Motokura, K.; Tada, M.; Iwasawa, Y. Heterogeneous organic base-catalyzed reactions enhanced by acid supports. *J. Am. Chem. Soc.* **2007**, *129*, 9540–9541.
- (44) Almeida, K. A.; Cardoso, D. Basic activity of Y zeolite containing alkylammonium cations in Knoevenagel condensation. *Catal. Today* **2013**, *213*, 122–126.
- (45) Motokura, K.; Tada, M.; Iwasawa, Y. Cooperative catalysis of primary and tertiary amines immobilized on oxide surfaces for one-pot C–C bond forming reactions. *Angew. Chem.* **2008**, *120*, 9370–9375.
- (46) Hara, T.; Kanai, S.; Mori, K.; Mizugaki, T.; Ebitani, K.; Jitsukawa, K.; Kaneda, K. Highly efficient C–C bond-forming reactions in aqueous media catalyzed by monomeric vanadate species in an apatite framework. *J. Org. Chem.* **2006**, *71*, 7455–7462.
- (47) Poe, S. L.; Kobašljia, M.; McQuade, D. T. Microcapsule enabled multicatalyst system. *J. Am. Chem. Soc.* **2006**, *128*, 15586–15587.
- (48) Shylesh, S.; Wagner, A.; Seifert, A.; Ernst, S.; Thiel, W. R. Cooperative acid–base effects with functionalized mesoporous silica nanoparticles: Applications in carbon–carbon bond-formation reactions. *Chem.—Eur. J.* **2009**, *15*, 7052–7062.
- (49) Zeidan, R. K.; Hwang, S. J.; Davis, M. E. Multifunctional heterogeneous catalysts: SBA-15-containing primary amines and sulfonic acids. *Angew. Chem., Int. Ed.* **2006**, *45*, 6332–6335.
- (50) Brunelli, N. A.; Didas, S. A.; Venkatasubbaiah, K.; Jones, C. W. Tuning cooperativity by controlling the linker length of silica-supported amines in catalysis and CO₂ capture. *J. Am. Chem. Soc.* **2012**, *134*, 13950–13953.
- (51) Sakthivel, K.; Notz, W.; Bui, T.; Barbas, C. F. Amino acid catalyzed direct asymmetric aldol reactions: a bioorganic approach to catalytic asymmetric carbon–carbon bond-forming reactions. *J. Am. Chem. Soc.* **2001**, *123*, 5260–5267.